ISSN 1392-1320 MATERIALS SCIENCE (MEDŽIAGOTYRA). Vol. XX, No. X. 2027

Study on the Acoustic Performance of a Novel Light Glass Wool-glass fiber mat Composite Material for Cabin Interior Acoustic Packaging of Electric Vehicles' Cockpits

Jintao SU [1], Weizheng LIU [1], Fengze LIU [1], Nenghui HUANG [2] *

[1] *College of Automotive and Electrical Engineering, Harbin Cambridge University, 239 Haping Road, Xiangfang District, Harbin 150000, China*
[2] *School of Mechanical and Automotive Engineering, Science and Technology College of Hubei University of Arts and Science, No. 28 Yinji East Street, Xiangcheng District, Xiangyang 441025, Hubei Province, China*

http://doi.org/10.5755/j02.ms.42725

Received 5 September 2025; accepted 20 February 2026

This study employs the transfer matrix method combined with numerical simulations based on the transfer matrix model and an impedance tube testing system to explore the correlation mechanism of acoustic parameters in Light Glass Wool-glass fiber mat composite materials. Through experimental testing, key parameters such as resistivity, tortuosity and porosity were regulated to quantitatively analyze their influence laws on the acoustic characteristics of the composite structure. This study discusses the data analysis process, formula derivation process and basic assumptions of the research. The research results show: First, regarding the tortuosity of glass fibers: At high frequencies (1850 Hz) in the sound absorption coefficient, when the tortuosity increases to 2.8, the sound absorption coefficient increases by 0.86 %. The main reason is that a higher tortuosity makes the spatial structure of glass fibers more complex. When high-frequency sound waves enter, more reflection and refraction occur on the fiber surface, prolonging the propagation path of sound waves inside the material and increasing the contact opportunity with fibers, thus absorbing more sound energy. Second, regarding the porosity of glass fibers: At low frequencies (50 Hz), when the porosity increases to 0.94, the sound absorption coefficient increases by 40.5 %, and the reflection coefficient decreases by 1.6 %. The main reasons are: reducing "rigid reflection" of materials, and materials with high porosity are more "porous". When low-frequency sound waves hit the material surface, more energy enters the pores instead of being directly reflected. The 1.6 % decrease in the reflection coefficient is precisely because the rigid reflection of sound waves on the material surface is reduced, and more sound waves are guided into the interior to participate in the absorption process. Optimizing "viscous loss" conditions: Low-frequency sound waves vibrate more slowly and require sufficient pore space for air molecules to friction with the fiber walls. The increase in porosity makes the air flow between fibers freer, increasing viscous resistance. Sound wave energy is more dissipated through friction between air and fibers, further enhancing the sound absorption coefficient (40.5 % increase). Third, regarding the air interlayer: As the thickness of the air interlayer increases, the action mechanism of the interlayer space on medium-high frequency sound waves changes. A thicker air interlayer provides more sufficient propagation paths and space for medium-high frequency sound waves. During the multiple reflections, refractions, and dissipations of sound waves in the interlayer, more medium-high frequency sound energy is absorbed and dissipated. Therefore, the medium-high frequency sound transmission loss significantly increases, resulting in a substantial reduction in the medium-high frequency sound energy that penetrates the interlayer and continues to propagate. Finally: This study theoretically provides an optimized design idea for wide-band sound-absorbing composite materials, offering key reference for solving automotive noise problems.

Keywords: composite materials, acoustic properties, numerical simulation, porous materials.

1. INTRODUCTION

The acoustic package of a general passenger car generally refers to a combination of acoustic components that could reduce the internal sound pressure, especially the sound pressure of airborne sound. For general passenger cars, the acoustic package mainly included the sound-absorbing components in the engine compartment, the sound-absorbing or sound-insulating components in the passenger compartment, the sound-absorbing and sound-insulating components in the trunk and various acoustic seals. The acoustic package of a vehicle was an important component that had an impact on the acoustic characteristics inside the vehicle. By using the acoustic package, not only could the noise level inside the vehicle be reduced, but also the acoustic quality within the vehicle could be adjusted to meet the psychological expectations of customers [1]. Multilayer composite materials, by virtue of the flexibility in structural design, have promoted innovations in basic theories and characterization technologies at the academic level. At the industrial level, they enable the optimization of performance, cost, and functionality. Meanwhile, they possess strategic values in the fields of sustainable development and national defense security, serving as a key bridge connecting scientific research and engineering applications.

Yuan et al [2] fabricated a model of a glass fiber reinforced plastic/epoxy composite cylindrical shell and

* Corresponding author: N. Huang
E-mail: *11947@hbuas.edu.cn*

studied its vibro-acoustic performance under external sound excitation through experiments and numerical simulations, the effectiveness of the numerical method was verified, on this basis, based on the genetic algorithm with the fiber layup angle and the shell thickness as the optimization objectives respectively with the average sound pressure value at the specified position inside the composite cylindrical shell at the resonance frequency and the mass of the model as the optimization objectives, the optimization was carried out, as a result, the low-frequency noise was suppressed and the weight was reduced by 32 %. Meng et al [3] have studied the sound absorption performance of the underwater resonant sound-absorbing materials by combining homogeneous materials with different resonance frequencies into a multi-layer composite sound-absorbing structure. The sound absorption frequency band was broadened by optimizing the structural dimensions and material parameters, achieving an efficient sound absorption effect in the low-frequency and wide-frequency range. Sascha et al [4] reduced the propulsive noise of the submarine propeller, the method combining the finite element method and the boundary element method was used fully considering factors such as stiffness, damping and mass, a cost function representing the total radiated sound power of the submarine was established, the optimization variables were determined through sensitivity analysis and the optimization solution was carried out with the minimization of the radiated sound power of the entire submarine as the optimization objective, thus controlling the radiated noise of the submarine. Farough et al. [5] have studied the damping characteristics of the viscoelastic sandwich composite cylindrical shell based on the genetic algorithm and the sequential quadratic programming algorithm by seeking the optimal parameters such as the interlayer interface characteristics. The thickness of the surface layer and the core material, the goal of maximizing the damping of the viscoelastic sandwich composite cylindrical shell was achieved. Xu et al [6] usd the boundary element technology, the topological optimization was carried out for the problem of minimizing the radiated sound power of the composite material plate, numerical examples showed that the maximum value of the radiated sound power was reduced by 20 dB, which verified the effectiveness of the optimization method, however, the problem was that as the frequency increases, the optimized topological structure became extremely complex and difficult to fabricate. Shojaei-fard et al. [7] had an exact solution to the vibration equation of the multilayer composite cylindrical shell and the acoustic wave equation was obtained based on the genetic algorithm with the maximization of the sound transmission loss of the symmetric multilayer composite cylindrical shell as the optimization objective, the layup angle and material type were optimized, under the same sound transmission loss, both the weight and the number of plies were reduced. Niu et al. [8] studied vibration and sound problems of the composite laminated plate under external loads, the Rayleigh integral was used to calculate the radiated sound power on the fluid-solid coupling surface, which was taken as the optimization objective function, the optimization analysis was carried out with the layup angle and material properties as the design variables. Abe et al. [9] used the boundary element method to study the geometric optimization design method of the sound insulation wall in order to avoid converging to the local solution near the initial value and introduced the topological derivative method, numerical examples showed that this method could obtain the optimized geometric structure without being affected by the initial values. Sassaf et al. [10] used the finite element method to analyze the fluid-solid coupling vibro-acoustic response characteristics of the damping sandwich plate structure in the fluid, meanwhile, the influences of geometric and material properties on the damping characteristics were analyzed, which were very beneficial to the implementation of the optimization research work. Foreign has conducted in-depth research in cutting-edge fields such as acoustic metamaterials, with a relatively solid theoretical foundation. For example, significant progress has been made in the theory of transformation acoustics. The design of novel acoustic structures has promoted the development of device-oriented applications.

Zhang et al. [11] analyzed the acoustic characteristics of the cab of a certain commercial vehicle, first, conducting an analysis of the acoustic structural mode participation factor and a panel contribution analysis for the sound pressure peak value at 81 Hz, carrying out free damping treatment on the panel with the greatest contribution, taking the relative density of the damping material unit as the design variable and taking the volume of the damping material as the constraint condition, taking the maximization of the modal damping ratio corresponding to the structural mode with the greatest contribution as the optimization objective, the usage amount of the damping material was optimized, the sound pressure at the right ear of the driver and the sound pressure at the right ear of the passenger were respectively reduced by 11.2 dBA and 10.7 dBA near 81 Hz. Fan et al. [12] had a method for calculating the surface acoustic impedance matrix by using the equivalent non-local impedance basic algebraic model was proposed for the problem of acoustic scattering of a rigid body coated with viscoelastic materials, taking a sphere coated with viscoelastic materials as an example, the parameters of the non-local acoustic impedance algebraic model were optimized by using the globally convergent moving approximation algorithm, so that the calculation results of acoustic scattering were consistent with those obtained by using the finite element method, it provided an effective way for studying the acoustic scattering of complex underwater targets such as submarines. Chen et al. [13] established an analytical relationship between the sound energy absorption rate and the size of the holes as well as the porosity and took the variation law of the size of the cylindrical holes along the thickness direction of the material as the design variable, carried out the optimization design research with the sound energy absorption rate of the layered porous structure at a specific frequency as the optimization objective and obtained a gradient porous structure with a relatively high sound energy absorption rate. Chen et al. [14] aimed at the problem of sound radiation of the composite material plate structure, taking parameters such as the layup angle, the number of layup layers and the sequence of the composite material as design variables and taking the radiated sound power as the optimization objective, the optimization analysis was carried out based

on the genetic algorithm, this effectively reduced the vibration and sound radiation of the structure and verifies the effectiveness of the optimization method. Wu [15] aimed at the layout optimization problem of the composite material wing surface structure. A two-level optimization design technique was proposed. The layout optimization problems of the composite material stiffened panel and the horizontal stabilizer of a certain type of aircraft were studied respectively, which verified the effectiveness and practicability of this method. Li et al. [16] used the adjoint method to obtain the sensitivity of the nodal displacements on the elastic plate to the damping layer elements, the variable density optimization method was employed to optimize the laying positions of the damping materials, meanwhile, the filtering formula proposed by Sigmund was introduced to suppress the checkerboard phenomenon that occurred during the optimization process, the research showed that compared with the uniform laying of damping materials, the structure with the optimized laying positions of damping materials could effectively suppress the sound pressure level at the control points in the acoustic cavity and reduced the structural weight. Domestically, notable achievements have been made in the research and development of novel acoustic materials, such as lightweight high-strength damping porous materials, with a focus on material environmental protection. The applied research in specific fields has been continuously deepened, and relevant work is carried out in line with domestic demands.

There is a gap between domestic and international advanced levels. In China, there are many repetitive products at the same or low level, while there are few products with high technical content. The technological equipment is backward, lacking special production equipment, and the large-scale production capacity is insufficient. There is a shortage of quality testing instruments and equipment. It is necessary to strengthen technological innovation, improve the technical content of products, improve process equipment, enhance the scale and automation level of production, and improve the quality detection system.

2. DERIVATION OF THEORETICAL FORMULAS

2.1. Transfer matrix method

Existing research shows that the acoustic properties of materials are closely related to their microstructural parameters. To this end, based on the theoretical framework of the transfer matrix method, an acoustic transmission model of composite multilayer materials is constructed in this study. By regulating key parameters such as the resistivity of Light Glass Wool (9000 $Nm^{-4}s$- 25000 $Nm^{-4}s$), the tortuosity of glass fiber mat (1.2 – 2.8) and the porosity (0.34 – 0.94). The loudspeaker generated a plane wave inside the impedance tube, as shown in Fig. 1. The width of the material under test was d, which divided the impedance tube into two sections: the upstream section and the downstream section. Four sensors were respectively placed at the upstream and downstream positions, the sound pressures at the corresponding positions from 1 to 4 can be measured, which were represented by P1 to P4 respectively [17]:

$$P_1 = Ae^{-jkx_1} + Be^{jkx_1}; \quad (1)$$

$$P_2 = Ae^{-jkx_2} + Be^{jkx_2}; \quad (2)$$

$$P_3 = Ce^{-jkx_3} + De^{jkx_3}; \quad (3)$$

$$P_4 = Ce^{-jkx_4} + De^{jkx_4}. \quad (4)$$

Among them, A and B were the sound pressure amplitudes at position 1, C and D were the sound pressure amplitudes at position 3, $k = \frac{2\pi f}{c_0}$ was the wave number and c_0 was the sound velocity in the air.

According to the transfer matrix function method, the expressions of coefficients A to D could be obtained respectively from the sound pressure results measured at positions 1, 2 and positions 3, 4 [17]:

$$A = \frac{P_1 e^{jks} - P_2}{e^{jks} - e^{-jks}}; \quad (5)$$

$$B = \frac{-P_1 e^{-jks} + P_2}{e^{jks} - e^{-jks}}; \quad (6)$$

$$C = \frac{P_3 e^{jks} - P_4}{e^{jks} - e^{-jks}}; \quad (7)$$

$$D = \frac{-P_3 e^{jks} + P_4}{e^{jks} - e^{-jks}}. \quad (8)$$

Homogeneous and isotropic porous materials can be described by an equivalent fluid model. For normally incident sound waves (Fig. 2), the sound field is characterized by the sound pressure P and the acoustic particle velocity V (m/s), where V denotes the velocity of air particles inside the porous medium. The relationship between the incident acoustic quantities (p_i, v_i) on the front surface and the transmitted quantities (p_t, v_t) on the rear surface is governed by the transfer matrix of the material layer [17]:

$$\begin{bmatrix} P \\ V \end{bmatrix}_{x=0} = \begin{bmatrix} T_{11} & T_{12} \\ T_{21} & T_{22} \end{bmatrix} \begin{bmatrix} P \\ V \end{bmatrix}_{x=d}. \quad (9)$$

The sound pressure and sound velocity information of the two surfaces of the material could be obtained from the coefficients A to D.

$$P_0 = Ae^{-jkx_1} + Be^{jkx_1}; \quad (10)$$

$$V_0 = \frac{Ae^{-jkx_1} - Be^{jkx_1}}{\rho_0 c_0}; \quad (11)$$

$$P_d = Ce^{jk(x_3-d)} + De^{-jk(x_3-d)}; \quad (12)$$

$$V_d = \frac{Ce^{jk(x_3-d)} - De^{-jk(x_3-d)}}{\rho_0 c_0}. \quad (13)$$

By changing the acoustic impedance at the right port of the impedance tube, N sets of linearly independent parameters can be obtained [17]. For each set, the sound pressures and particle velocities measured at the front surface (x = 0) and rear surface (x = d) are respectively denoted as $[P_1 \quad P_2 \quad \cdots \quad P_N]^T_{x=0}$, $[V_1 \quad V_2 \quad \cdots \quad V_N]^T_{x=0}$ and $[P_1 \quad P_2 \quad \cdots \quad P_N]^T_{x=d}$, $[V_1 \quad V_2 \quad \cdots \quad V_N]^T_{x=d}$. These vectors constitute the input data for determining the transfer matrix elements.

In fact, only the data of the sound pressure and sound velocity on the front and rear surfaces of the material under two kinds of acoustic impedance conditions needed to be measured and then the characteristics of the material transfer matrix could be obtained. For multi-layer materials, the transfer matrices of each layer of material could be combined into a total transfer matrix.

$$[T] = [T_1][T_2] \cdots \cdots [T_N]. \quad (14)$$

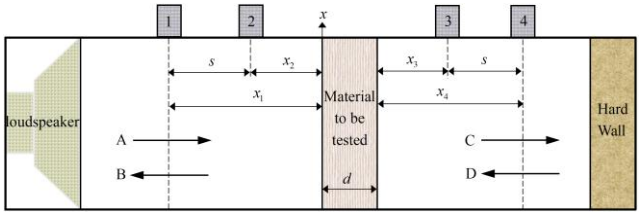

Fig. 1. Test diagram of the impedance tube

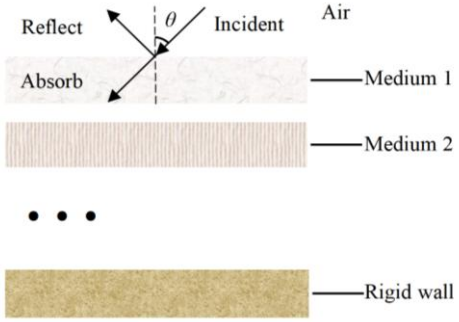

Fig. 2. Model of composite multilayer materials

The primary computational objective of the transfer matrix model is to calculate the sound pressure (P) and particle velocity (V) at the front and rear surfaces of the material. The raw calculated results of P and V are not explicitly presented in this paper, as the study focuses on the acoustic metrics derived from these two fundamental physical quantities, metrics that are directly comparable with the experimental measurements obtained via the impedance tube, namely the sound absorption coefficient, characteristic impedance, and reflection coefficient. All numerical simulation results presented in Chapter 4 are based on these derived acoustic metrics and have been systematically compared and validated against the impedance tube experimental data under identical parameter configurations. The excellent agreement observed between the derived acoustic metrics and experimental measurements fully substantiates the accuracy and reliability of the transfer matrix model in calculating P and V.

3. EXPERIMENTAL STUDY ON ACOUSTIC PROPERTIES OF COMPOSITE MATERIALS

3.1. Experimental parameter settings

Condition settings for multilayer composite materials (lightweight glass wool-glass fiber mat):

1. Experimental objectives: to verify whether the theoretical model holds for predictions in different frequency bands;
2. Independent variables: resistivity, tortuosity, porosity.
3. Dependent variables: effects of light glass wool-glass fiber mat composite structural parameters on acoustic properties, measured via independent variables.

The test ranges of the degree of resistivity of light glass wool are 9000 $Nm^{-4}s$, 15000 $Nm^{-4}s$ and 25000 $Nm^{-4}s$. The test ranges of the tortuosity of the glass fiber mat are 1.2, 1.9 and 2.8. The test ranges of the porosity are 0.34, 0.64 and 0.94.

Tortuosity and porosity are dimensionless parameters used to characterize porous media. Tortuosity, which quantifies the geometric complexity of a porous network, is defined as the square of the ratio of the effective propagation path length to the straight-line distance through the material. Porosity refers to the volume fraction of void spaces in a porous medium, ranging from 0 (a fully dense solid) to 1 (a perfectly porous medium).

The reasons for selecting the multi-layer material of lightweight glass wool-glass fiber are as follows: the combination of their "lightweight + multi-functional" characteristics can meet the multiple demands of weight reduction, noise reduction, and thermal insulation in construction, industry, transportation and other fields. Meanwhile, considering both economy and durability, it is an optimal solution among composite materials.

3.2. Experimental apparatus and test methods

This research utilizes the impedance tube technique to evaluate the acoustic characteristics of composite materials. The experimental configuration and testing protocols follow the approach delineated by Su et al. [18] in their investigation of acoustic packaging optimization for electric vehicle motor compartments. All measurements were performed in strict compliance with the ISO 10534-2 standard, employing a dual-microphone impedance tube apparatus, depicted in Fig. 3, Fig. 14 [18]. Test specimens with a diameter of 29 mm were examined over a frequency range spanning 10 to 6000 Hz, enabling a comprehensive assessment of the materials' acoustic behavior across low to high frequencies. This methodology is advantageous due to its minimal sample size requirements, high accuracy, and strong reproducibility, rendering it well-suited for systematic comparative analyses of multilayer composite materials under controlled experimental conditions.

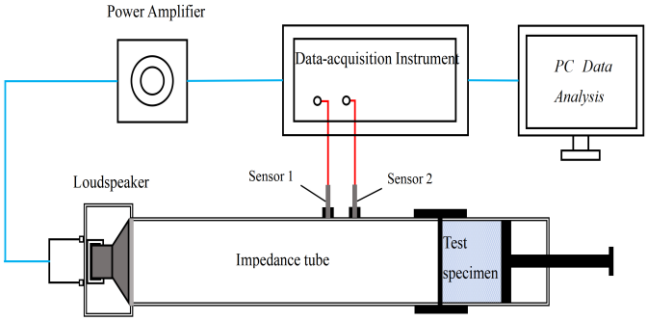

Fig. 3. Schematic diagram of the impedance tube experiment principle [18]

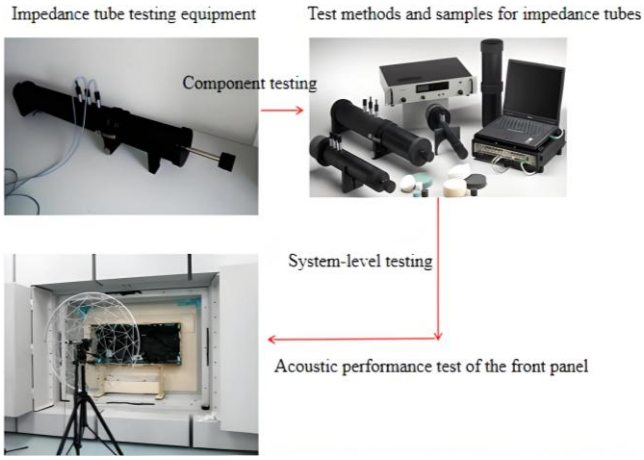

Fig. 4. Component testing and system testing methods for acoustic package materials [18]

A numerical simulation study was performed to analyze the acoustic properties of unreinforced fiber-class porous flexible glass wool, utilizing the transfer matrix model. The input parameters for the simulation, corresponding to this material, are presented in Table 1.

Table 1. Input parameters for material simulations

Material parameter	Unreinforced fiberglass-5.5 kg/m^3	Porous flexible glass wool
Porosity	0.94	0.99
Flow resistivity	20000	9000
Tortuosity	1.2	1.0
Viscous characteristic length, m	5.2×10^{-5}	1.92×10^{-4}
Thermal characteristic length, m	1.04×10^{-4}	3.84×10^{-4}
Solid density, kg·m^3	5.5	16
Poisson ratio	0	0

The frequency range considered spans from 50 Hz to 5000 Hz. The excitation was implemented using plane wave excitation, while the boundary condition at the rear surface was modeled as a rigid wall.

3.3. Theoretical analysis of experimental results

When the resistivity was 9000 N·m^{-4}·s, the sound absorption coefficient of the material was 0.077 at 50 Hz and reached the first peak of 0.996 at 1050 Hz. As the resistivity increased to 25000 N·m^{-4}·s, the sound absorption coefficient at 50 Hz increased to 0.135, indicating that a higher resistivity improves low-frequency performance. The tortuosity increased with the frequency and showed a positive correlation with the sound absorption coefficient. A higher porosity enhanced low-frequency sound absorption but slightly reduced high-frequency absorption.

When the real part of resistivity was 9000 N·m^{-4}·s, it increased with frequency in the high-frequency band. For 15000 N·m^{-4}·s and 25000 N·m^{-4}·s, the real part rose slowly with frequency, showing overall better stability. In the mid-frequency band, the real part of sound impedance with tortuosity 2.8 was higher than that with tortuosity 1.2 and 1.9. The porosity showed a gradual increase trend in the high-frequency band as the frequency increased.

When the resistivity was 9000 N·m^{-4}·s, the real part was high and the absolute value of the imaginary part was low, leading to strong low-frequency reflection and weak high-frequency reflection, which was suitable for sound absorption in the mid-high frequency range. For 15000 N·m^{-4}·s, the absolute value of the imaginary part reached a peak. In the low-frequency band, the tortuosity decreased with increasing frequency and showed a negative correlation with the reflection coefficient. In the low-frequency band, the real part of porosity decreased with increasing frequency.

4. SIMULATION RESULTS

4.1. Analysis of the influence of the resistivity of light glass wool-glass fiber mat composite materials on acoustic characteristics

The test ranges of the degree of resistivity of light glass wool are 9000 Nm^{-4}s, 15000 Nm^{-4}s and 25000 Nm^{-4}s. The three groups of test diagrams are as follows. The first group is shown in Fig. 5. The second group is shown in Fig. 6. The third group is shown in Fig. 7.

As shown in Fig. 5, in the low-frequency band, the resistivity showed a continuous upward trend with the gradual increase of frequency. Due to the positive correlation between resistivity and sound absorption coefficient, the material exhibited stronger sound energy loss. In the mid-high frequency band, all flow resistivities decreased with the increase of frequency, leading to weaker sound energy loss in the material. Thus, sound waves were less likely to be absorbed but had stronger penetrating ability.

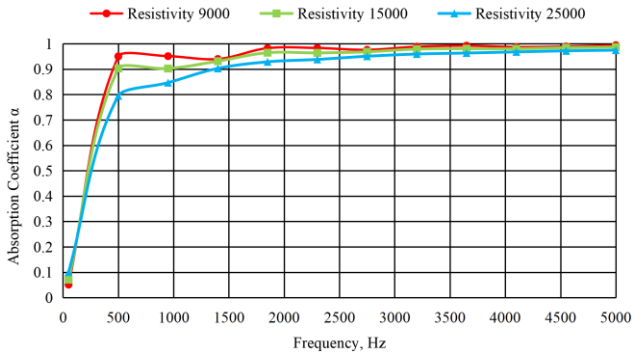

Fig. 5. Influence of the resistance of light wool on the absorption coefficient

As indicated by Fig. 6, in the low-frequency band, as the frequency increased, the resistivity rose, enhancing the material's sound energy absorption. The attenuation of sound energy during propagation became more pronounced, and the ability of sound waves to penetrate the material gradually weakened. The material's resistance to sound energy increased, causing more sound energy to be absorbed and converted into other forms of energy, which exacerbated the degree of sound energy loss.

The real component of the electrical resistivity quantifies a material's ability to dissipate energy from incident sound waves. Fundamentally, this energy dissipation arises from viscous friction between air molecules and fiber surfaces, as well as thermal conduction

among air molecules during sound wave propagation within the material.

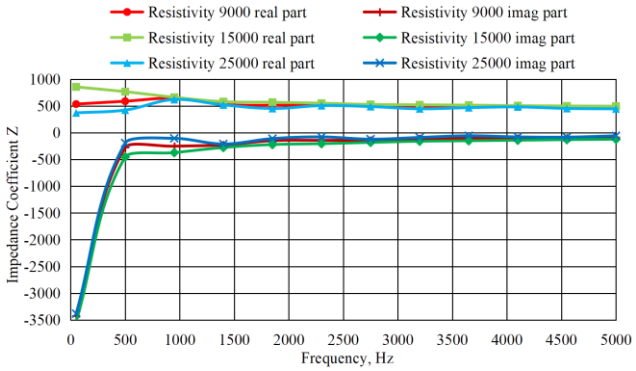

Fig. 6. Influence of the resistance of light glass wool on the impedance

A larger real component corresponds to a higher efficiency of converting acoustic energy into other forms (e.g., thermal energy), thus improving the material's sound absorption performance.In contrast, the imaginary component describes the inertial properties of the material and characterizes the phase change of sound waves propagating through porous media. Its magnitude directly affects the reflection and transmission coefficients of sound waves at the material interface.

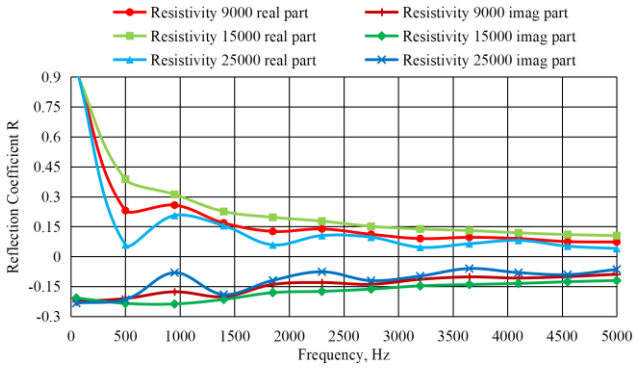

Fig. 7. Influence of the resistance of light glass on the reflection coefficient

As shown in Fig. 7, at 9000 $N \cdot m^{-4} \cdot s$, sound wave reflection dominated in the low-frequency band with strong reflected energy, while the reflection effect weakened significantly in the high-frequency band, making sound waves more susceptible to absorption. Based on this characteristic, such materials exhibit significant advantages in mid-high frequency sound absorption. The real part of 9000 $N \cdot m^{-4} \cdot s$ was high and the absolute value of the imaginary part was low, leading to strong low-frequency reflection and weak high-frequency reflection-suitable for mid-high frequency sound absorption. The absolute value of the imaginary part reached a peak at 15000 $N \cdot m^{-4} \cdot s$, where the material showed stronger acoustic resistance in the low-frequency band. This made low-frequency sound waves difficult to penetrate, thereby enhancing the reflection effect in the low-frequency range.

Based on the transfer function method, an impedance tube was used to test the sound absorption characteristics of the headliner material. The resistivity of the headliner material was tested based on the direct current air flow method and the influences of the production process, fabric, PU, glue and flow resistivity on the headliner were analyzed. The average absorption coefficient increased with the increase of the resistivity. Reasonably selecting a headliner with a higher resistivity could effectively increase the resistance to the propagation of sound waves in the material, which was conducive to the rapid attenuation of sound energy and the improvement of the sound absorption effect [19]. The cited literature proposes that "the average absorption coefficient increased with the increase of the resistivity", but it does not clarify the specific performance in the high-frequency band. This study, by covering a wide frequency band from 50 Hz to 5000 Hz, reveals the high-frequency absorption advantage of light glass wool under 25000 $Nm^{-4}s$. At 4550 Hz, the absorption coefficient is 0.971, which is close to the ideal sound absorption effect (1.0). The absorption coefficient is 0.975 at 5000 Hz, indicating that the material still maintains good performance in the high-frequency band.

4.2. Analysis of the influence of the tortuosity of light glass wool-glass fiber mat composite materials on acoustic characteristics

The test ranges of the degree of tortuosity of glass fiber mat are 1.2, 1.9, and 2.8. The three groups of test diagrams are as follows. The first group is shown in Fig. 8. The second group is shown in Fig. 9. The third group is shown in Fig. 10.

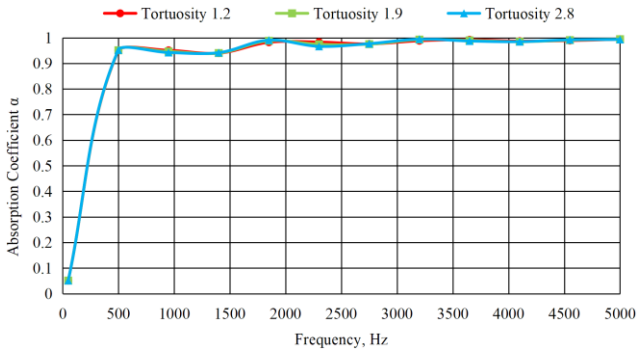

Fig. 8. Influence of the tortuosity of the glass fiber mat on the absorption coefficient

As revealed by Fig. 8, in the low-frequency band, the tortuosity of the material continuously increased as the frequency rose. Given the positive correlation between tortuosity and sound absorption coefficient, a higher frequency implies greater material tortuosity, enhancing sound energy absorption. This leads to a higher proportion of sound energy converted into other forms, resulting in a more significant loss. In this frequency range, low-frequency sound waves exhibit relatively small energy loss and easier propagation due to lower tortuosity. Entering the mid-high frequency band, the growth trend of tortuosity flattened, no longer increasing significantly with frequency. This limits the increase in the material's sound absorption coefficient and slows the rate of sound energy loss. Compared with the low-frequency band, although mid-high frequency sound waves have higher frequencies, the sound energy absorption and loss do not change significantly due to the lack of significant tortuosity increase. Thus, the ability of sound waves to penetrate the material remains relatively

stable, without severe attenuation caused by frequency increase.

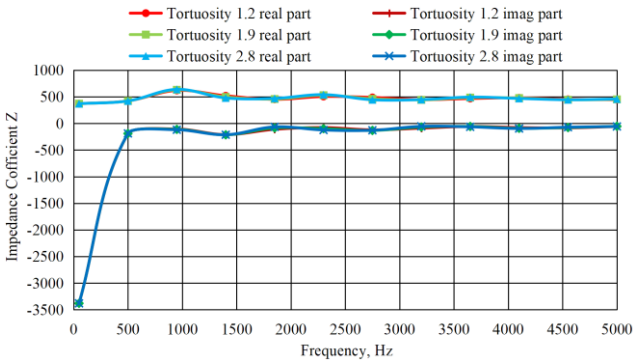

Fig. 9. Influence of the tortuosity of glass fiber mat on the impedance

As shown in Fig. 9, the material with tortuosity 2.8 more strongly impedes sound wave propagation in the mid-frequency band. When sound waves contact such materials, more energy is absorbed and dissipated, significantly weakening the waves' penetration ability and enhancing sound energy attenuation. In contrast, materials with lower tortuosity impose relatively minor resistance to sound energy, leading to limited energy loss.

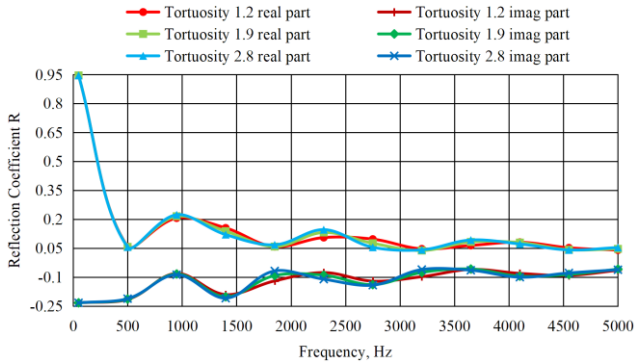

Fig. 10. Influence of the tortuosity of the glass fiber mat on the reflection coefficient

As indicated by Fig. 10, in the low-frequency band, as the frequency increased, the tortuosity decreased and the reflection coefficient increased, enhancing sound wave reflection on the material surface. More sound energy was reflected to the original medium, reducing the energy penetrating the material for further propagation. Meanwhile, increased reflection led to less sound energy being absorbed and converted into other forms within the material, weakening the overall degree of sound energy loss.

Based on the theoretical model of the absorption coefficient of multilayered porous materials and the tabu algorithm, the porosity, tortuosity, viscous c.d and thermal c.d of the porous materials were optimized and solved. Substituting the parameters obtained through back calculation into the simulated acoustic package of the vehicle-level Statistical Energy Analysis (SEA) model, the vehicle-level Acoustic Transfer Function (ATF) were calculated and conducted an analysis in combination with the test. It could be seen from the test results that based on the theoretical model of the multilayer system of porous materials and combined with the optimization algorithm, relatively accurate parameters could be deduced inversely, which also illustrated the effectiveness of the method. Aiming at the multi-factor optimization problem of the acoustic package, a method for optimizing the acoustic package by combining the analysis of variance with the response surface model was proposed. First, obtaining the significant influencing factors of the acoustic package performance through the range analysis and analysis of variance. Then, constructing the response surface model between the factors with higher significance levels and the sound pressure level of the acoustic cavity at the driver's head. Genetic algorithm optimization was carried out under the constraints of thickness and mass. After optimization, the sound pressure level of the acoustic cavity at the driver's head was reduced by 0.66 dB(A), and the mass of the acoustic package was decreased by 0.93 kg (that was reduced by 23.97 %) [20]. The cited literature improves the acoustic performance by optimizing multiple parameters such as porosity, tortuosity, viscous c.d, etc. However, it fails to analyze the independent role of the degree of tortuosity separately. In this study, by adjusting the degree of tortuosity, it is revealed when the degree of tortuosity is 1.9, the absorption coefficient is 0.99 at 5000 Hz, which is close to the ideal value. The negative value of the theoretical values of the reflection coefficient decreases with the increase of the degree of tortuosity, indicating that a high degree of tortuosity optimizes the phase matching and reduces the reflection of high-frequency standing waves.

4.3. Analysis of the influence of the porosity of light glass wool-glass fiber mat composite materials on acoustic characteristics

The test ranges of the porosity of glass fiber mat are 0.34, 0.64 and 0.94. The three groups of test diagrams are as follows. The first group is shown in Fig. 11. The second group is shown in Fig. 12. The third group is shown in Fig. 13.

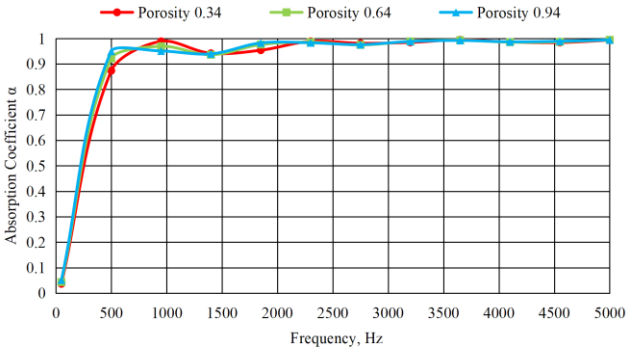

Fig. 11. Influence of the porosity of the glass fiber mat on the absorption coefficient

As shown in Fig. 11, in the low-frequency band, as the frequency increased, the porosity increased, significantly enhancing the material's sound energy absorption capacity. The energy dissipation of sound waves within the porous structure became more pronounced, leading to a substantial reduction in sound energy penetrating the material and more significant sound energy attenuation. The increase in spatial structures within the material that allow sound waves to reflect, refract, and friction resulted in more sound energy

being converted into other forms of energy, such as heat within the pores, thereby exacerbating sound energy loss.

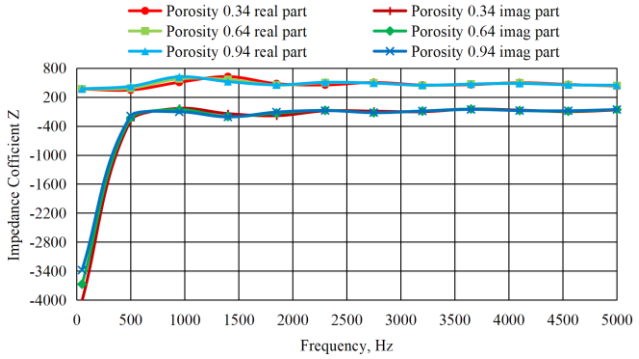

Fig. 12. Influence of the porosity of the glass fiber mat on the impedance

As shown in Fig. 12, due to the slow growth of porosity, the material's ability to absorb and dissipate sound energy through the porous structure was limited. Thus, the increase in sound energy loss with frequency was relatively small, without significant exacerbation. With the gentle change in porosity, the efficiency of sound energy conversion into other forms within the pores remained nearly constant, leading to a stable rate of sound energy attenuation. The ability of sound waves to penetrate the material did not drop sharply with frequency increase.

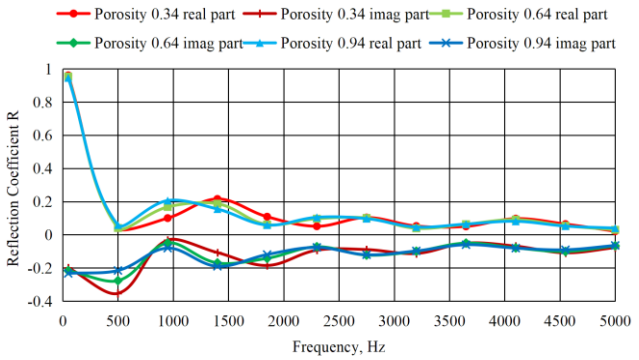

Fig. 13. Influence of the porosity of the glass fiber mat on the reflection coefficient

As shown in Fig. 13, in the low-frequency band, when the frequency was low and the real part of porosity was small, the reflection coefficient was high. Most sound energy was reflected by the material surface, with limited energy entering the material for absorption, leading to restricted sound energy loss. At a porosity of 0.94 in the high-frequency band (4550 – 5000 Hz), the real part of the reflection coefficient was below 0.05, and the negative value of the imaginary part decreased, indicating simultaneous suppression of sound energy reflection and optimization of phase matching.

The effect of porosity on the mechanical properties of composites made from brittle, particulate matrices had been studied using glass fibre-reinforced gypsum plaster as the model. Composite boards were prepared by the spray-suction method, which produced a random two-dimensional arrangement of the chopped fibre in the matrix. Variation in the porosity occurred as a result of changing the proportion and length of the reinforcement. Beyond optimum fibre volume percentages, both tensile and bending strengths of the glass fibre-reinforced gypsum plaster decrease and this reduction was related to the increase in porosity which accompanies the addition of relatively large quantities of a fibrous material to a particulate matrix. The effect on porosity of a change in fibre length was less pronounced and was only significant for lengths exceeding 22 mm. Impact strength had been found to increase with both fibre length and fibre content up to the limits that were investigated. An attempt had been made to relate the porosity of the composite (over the range 20 to 40 %) with the efficiency of reinforcement by discontinuous fibres. The shape of the tensile stress-strain curve could be explained in terms of this relationship [21]. The cited literature focuses on the influence of porosity on mechanical properties and this study establishes a refined correlation between porosity and acoustic properties. In the low-frequency range, the increase of the porosity to 0.94 is accompanied by an increase in the absorption coefficient, indicating that a high porosity enhances the absorption of low-frequency noise.

4.4. Double-sided wall structure

Condition settings: Wall 1 – aluminum shell; Wall 2 – aluminum with honeycomb structure; variables of inner cavity width: 0.5 m, 0.8 m, and 1 m (denoted by w); rear boundary condition: fluid domain; excitation mode: diffuse field; frequency range: 50 – 5000 Hz; composite material: light glass wool-glass fiber mat.

The double-sided wall structure model is shown in Fig. 14.

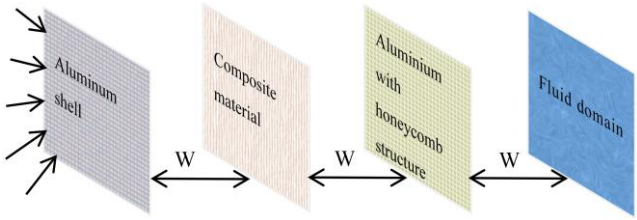

Fig. 14. Double-sided wall structure model

Based on the transfer matrix method employed in our previous study [17], the theoretical Analysis of Experimental Results were performed. As the thickness of the air interlayer decreases from 1 m to 0.5 m, the decibel (dB) value gradually increases from 19.913 dB to 22.357 dB in the low-frequency range, indicating a negative correlation between the air interlayer thickness and the dB value. Specifically, a smaller air interlayer thickness corresponds to a higher dB value in the low-frequency band. In the low-frequency range, there is a negative correlation between the thickness of the air interlayer and the decibel value (i.e., a decrease in thickness leads to an increase in decibel value). The main reasons can be analyzed from two aspects: acoustic principles and structural characteristics.

I. Core reasons: propagation characteristics of low-frequency sound waves and sound insulation mechanism of the interlayer. Long wavelength characteristics of low-frequency sound waves: low-frequency sound waves have longer wavelengths (e.g., the wavelength of a 100 Hz sound wave is approximately 3.4 meters). When the thickness of the air interlayer decreases from 1 meter to 0.5 meters, the ratio of the interlayer thickness to the low-frequency wavelength decreases, resulting in insufficient “blocking

space" of the interlayer for low-frequency sound waves. In this case, sound waves are more likely to be directly transmitted through air vibration in the interlayer, making it difficult to achieve effective attenuation (such as resonance suppression or energy dissipation). Influence of resonance effect: the air interlayer can be regarded as an "acoustic resonance cavity", and its natural frequency is related to its thickness (the smaller the thickness, the higher the natural frequency). When the thickness of the interlayer decreases, its natural frequency may be closer to the frequency of the low-frequency sound source, causing resonance, which in turn amplifies the sound wave energy and leads to an increase in the transmitted decibel value.

II. Multi-aspect considerations: materials and boundary conditions. If the structures on both sides of the interlayer (such as walls and plates) have insufficient rigidity, a decrease in thickness will aggravate the transmission of structural vibrations, further weakening the sound insulation effect. Conversely, if the boundary materials have excellent sound insulation performance, this negative correlation may be weakened, but air transmission still dominates in the low-frequency range. Practical application scenarios. In building sound insulation (such as walls and floors), low-frequency noise (such as mechanical vibration and traffic noise) is inherently difficult to block. If the thickness of the air interlayer is limited (such as in small apartment decoration), it is necessary to use sound-absorbing materials (such as porous cotton) or damping structures to make up for the sound insulation loss caused by the reduced thickness.

Limitations of frequency range. This conclusion only applies to the low-frequency range. In the mid-to-high frequency range, the impact of a decrease in the thickness of the air interlayer may be different (e.g., high-frequency sound waves have shorter wavelengths, and a thinner interlayer may attenuate sound waves through reflection). Therefore, analysis should be conducted in combination with specific frequencies. In summary, the sound insulation effect of the air interlayer in the low-frequency range depends on sufficient thickness to match the long-wavelength characteristics. A decrease in thickness will lead to a decline in sound insulation performance due to insufficient space and resonance effects. In practical applications, comprehensive optimization should be carried out in combination with materials and scenarios.

In the mid-high frequency range (e.g., 1050 – 4550 Hz), taking 1050 Hz as an example, when the air interlayer thickness decreases from 1 m to 0.5 m, the dB value first decreases slightly (from 53.692 dB for a 1 m interlayer to 53.661 dB for a 0.8 m interlayer) and then increases slightly (to 54.174 dB for a 0.5 m interlayer). Overall, the variation in dB values is minimal, suggesting that the thickness of the air interlayer has a negligible effect on the dB value in the mid-high frequency range. In the mid-to-high frequency range (1050 ~ 4550 Hz), changes in the thickness of the air interlayer have a minor and fluctuating impact on the decibel value (slightly decreasing first and then slightly increasing). This phenomenon is closely related to the propagation characteristics of mid-to-high frequency sound waves and the sound insulation mechanism of the interlayer. The specific reasons and considerations are as follows:

I. Core reasons: characteristics of mid-to-high frequency sound waves and weakened role of the interlayer. Short wavelength and dominance of reflection attenuation: mid-to-high frequency sound waves have shorter wavelengths (e.g., the wavelength of a 1050Hz sound wave is approximately 0.32 meters). When the interlayer thickness decreases from 1 meter to 0.5 meters, the thickness remains greater than or close to the wavelength of mid-to-high frequency sound waves. At this point, sound waves are more likely to be reflected by the interfaces on both sides of the interlayer (such as walls), and the proportion of energy attenuated through reflection is relatively high, thus weakening the impact of the "spatial thickness" of the air interlayer on sound insulation. Balance between resonance and energy dissipation: The natural frequency in the mid-to-high frequency range is relatively high, and the resonance effect of the air interlayer is weak (since the natural frequency of the interlayer increases with the decrease in thickness, resulting in a low degree of overlap with the frequency of mid-to-high frequency sound waves). When the thickness decreases from 1 meter to 0.8 meters, it may temporarily avoid the resonance point, leading to a slight decrease in the decibel value. However, when the thickness further decreases to 0.5 meters, the ratio of the interlayer thickness to the wavelength becomes too low, reducing the reflection efficiency. A small amount of sound waves are transmitted through air vibration, causing a slight rebound in the decibel value, but the overall fluctuation range is limited. Influence of air absorption: the energy dissipation of mid-to-high frequency sound waves in the air (such as molecular friction) is more significant. Even if the interlayer thickness changes, the absorption effect of air itself on mid-to-high frequency sound waves can partially offset the impact of thickness changes, resulting in small overall fluctuations in the decibel value.

II. Multi-aspect considerations: dominant role of materials and interfaces. Sound insulation in the mid-to-high frequency range relies more on the sound insulation performance of materials on both sides of the interlayer (such as the density and surface hardness of plates). If the materials have strong reflection capabilities for mid-to-high frequencies, the impact of thickness changes will be masked. If there are gaps or vibrations in the materials, local fluctuations may be amplified, but the overall situation remains stable. Differences in frequency subdivision, 1050Hz belongs to the lower limit of the mid-to-high frequency range, close to the low-frequency range, so the impact of thickness changes is slightly more obvious. In higher frequencies such as 4550 Hz, the wavelength is shorter (approximately 0.075 meters), and the interlayer thickness (0.5~1 meter) is much larger than the wavelength, resulting in stable reflection attenuation. Thus, the impact of thickness changes may be even weaker or even negligible.

Optimization directions in practical applications. The key to sound insulation for mid-to-high frequency noise (such as human voices and electrical noise) does not lie in the thickness of the air interlayer, but in reducing gaps (such as sealing doors and windows) and enhancing the sound absorption performance of materials (such as using porous materials to absorb mid-to-high frequencies). Even if the interlayer thickness changes, the sound insulation effect can be maintained by optimizing the sealing performance of interfaces. In summary, the thickness of the air interlayer has little impact on sound insulation in the mid-to-high

frequency range. This is because the short wavelength makes reflection attenuation dominant, and air absorption and material properties weaken the role of thickness. In practical applications, there is no need to over-rely on the interlayer thickness; instead, emphasis should be placed on material selection and interface treatment.

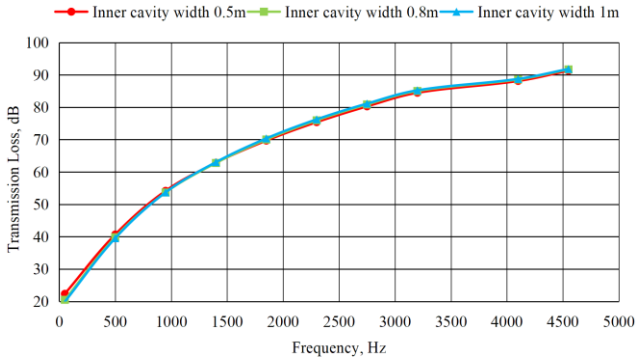

Fig. 15. Effect of different inner cavity width

It can be seen from Fig. 15, low-frequency band (e.g., 50 Hz): when the air cavity thickness is 1 m, the value is 19.913 dB; when it is 0.8 m, the value is 20.5 dB; and when it is 0.5 m, the value is 22.357 dB. It can be seen that the thinner the air cavity, the relatively higher the low-frequency transmission loss. Because the wavelength of low-frequency sound is longer, the "spring-vibration reduction" effect of the thin air cavity (the air layer is similar to an elastic body connecting the double plates to weaken the vibration transmission) is more easily matched and takes effect at low frequencies, so that more sound energy is reflected or absorbed. Mid-to-high-frequency band (e.g., 1050 – 4550 Hz): taking 1050 Hz as an example, for the 1 m air cavity, the value = 53.692 dB; for the 0.8 m air cavity, the value = 53.661 dB; and for the 0.5 m air cavity, the value = 54.174 dB.

Overall, the thicker the air cavity, the higher the mid-to-high-frequency transmission loss. A thick air layer can make more effective used of "elastic vibration reduction + sound wave refraction/scattering". When mid-to-high-frequency sound waves are incident, the elastic deformation of the thick air layer and the longer propagation path of sound waves in the air layer lead to more energy attenuation; at the same time, the refraction and scattering effects of sound waves at the air-wall interface are more significant, reducing the sound energy transmitted to the other side and improving the transmission loss. The transmission loss values fluctuate at different frequencies, which may be related to the "coincidence effect" (when sound waves are obliquely incident, the bending vibration of the wall surface matches the sound wave propagation, resulting in a sound insulation valley). The thickness of the air cavity affects the inherent vibration characteristics of the double-wall. A thick cavity (1 m) may shift the coincidence effect frequency or make the valley shallower, to a certain extent improving the mid-to-high-frequency sound insulation stability; a thin cavity (0.5 m) is prone to more obvious resonance or coincidence effects at some frequencies, resulting in fluctuations in transmission loss. The condition is a diffuse field.

It can be seen from Fig. 16, the width of the air gap affects the absorption and transmission of sound energy by altering the mass and stiffness distribution of the structure.

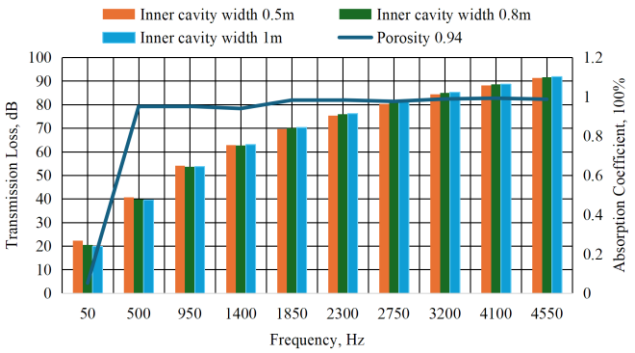

Fig. 16. Comparison between transmission loss and absorption coefficient

In terms of transmission loss, the width influences the attenuation of transmitted sound energy; in terms of the absorption coefficient, it affects the internal sound absorption mechanisms of the structure (such as the viscous damping of air), thereby changing the proportion of absorbed sound energy.

When the porosity is 0.94, the material contains a large number of pores, which provide channels for sound energy absorption. When sound waves strike the material surface, they enter the interior of the pores. During propagation within the pores, sound energy is dissipated as heat due to effects such as air viscosity and thermal conduction, leading to an increase in the absorption coefficient. Meanwhile, the pore structure within the material also impedes the propagation of sound waves, reducing transmitted sound energy and increasing transmission loss. Changes in porosity directly affect the pore distribution and connectivity within the material, thereby altering its acoustic properties.

It can be seen from Fig. 17, the width of the air gap alters the acoustic impedance and natural frequency of the structure, thereby influencing the reflection and transmission of sound energy.

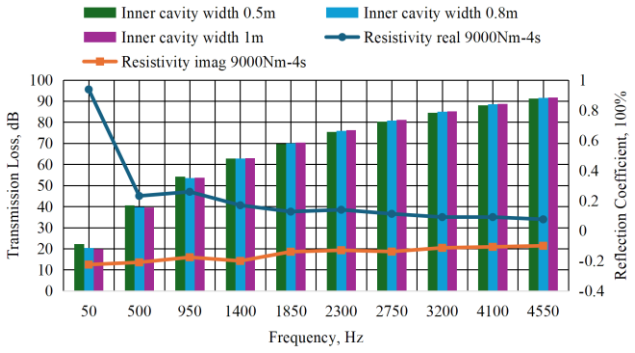

Fig. 17. Comparison between transmission loss and reflection coefficient

For transmission loss, the width affects the structure's ability to block sound energy; for the reflection coefficient, it impacts the structure's capacity to reflect sound energy. Although both mechanisms are related to the structural acoustic properties, their specific influencing modes and focuses differ.

The real of the flow resistivity is primarily associated with sound energy dissipation in the material. A larger real indicates more pronounced friction and viscous effects within the material, leading to greater energy dissipation

during sound propagation. This results in increased transmission loss and reduced reflection coefficient, as more sound energy is dissipated internally rather than reflected or transmitted. The image of the flow resistivity is related to the material's inertial effects, etc. Changes in the image affect the dynamic acoustic characteristics of the material, thereby influencing transmission loss and reflection coefficient. When the imaginary part of the flow resistivity changes, the material's response to sound waves at different frequencies also changes, causing the values of transmission loss and reflection coefficient to vary across frequency bands.

5.CONCLUSIONS

Based on experimental characterization and theoretical modeling, this study systematically investigates the structure-acoustic property relationships of lightweight glass wool-unreinforced fiberglass composite materials. The key findings are summarized as follows:

1. This work provides the first quantitative elucidation of the influence of microstructural parameters on broadband acoustic performance. Through precise control of flow resistivity, tortuosity, and porosity, the study establishes clear correlations between these parameters and sound absorption/insulation properties across a wide frequency spectrum (50 – 5000 Hz). Notably, increasing porosity to 0.94 enhances the low-frequency (50 Hz) sound absorption coefficient by 40.5 %, while elevating tortuosity to 2.8 improves the high-frequency (1850 Hz) absorption coefficient by 0.86 %. These findings offer critical theoretical guidance for the performance-oriented design of advanced acoustic materials.
2. A frequency-dependent reversal effect of air interlayer thickness on sound transmission loss (TL) is identified, representing a conceptual advancement. Challenging the conventional paradigm that “greater thickness yields superior insulation,” this study demonstrates that in the low-frequency regime (e.g., 50 Hz), a thinner air interlayer (0.5 m) yields higher TL (2.357 dB), attributable to enhanced spring-damping effects. In contrast, variations in interlayer thickness exhibit negligible influence on mid-to-high-frequency TL. This phenomenon provides a novel design strategy for low-frequency noise mitigation in spatially constrained environments such as electric vehicle cockpits.
3. An innovative co-design strategy termed “high-frequency absorption dominated by porosity, low-frequency absorption governed by tortuosity” is proposed. By leveraging frequency-dependent parameter dominance, this approach enables simultaneous enhancement of broadband sound absorption and insulation within a single lightweight composite material. This effectively addresses the longstanding challenge of balancing wideband acoustic performance in traditional materials, demonstrating significant potential for engineering applications.

In summary, this research not only establishes a theoretical framework for the optimized design of broadband sound-absorbing composites, but also provides a material design methodology addressing critical challenges in automotive NVH management, particularly in the context of lightweight and electric vehicle development.

Acknowledgments

Supported by Program for young talents of basic research in universities of Heilongjiang province (YQJH2024053).

REFERENCES

1. **Deng, J., Song, J., Li, C., Zhang, B.** Research on Design, Development and Optimization Technology of Acoustic Package for Passenger Cars *Acoustic Technology* 34 (4) 2015: pp. 353 – 357. https://doi.org/10.16300/j.cnki.1000-3630.2015.04.012
2. **Yuan, C., Roozen, N.B., Bergsma, O., Beukers, A.** Experimental-numerical Study and Optimization of Sound Insulation of a Finite Composite Cylinder *Engineering Analysis with Boundary Elements* 37 (2) 2013: pp. 250 – 259. https://doi.org/10.1016/j.enganabound.2012.09.013
3. **Meng, H., Wen, J., Zhao, H., Wen, X.** Optimization of Locally Resonant Acoustic Metamaterials on Underwater Sound Absorption Characteristics *Journal of Sound and Vibration* 331 (20) 2012: pp. 4406 – 4416. https://doi.org/10.1016/j.jsv.2012.05.027
4. **Merz, S., Kessissoglou, N., Kinns, R., Marburg, S.** Minimisation of the Sound Power Radiated by a Submarine Through Optimisation of its Resonance Changer *Journal of Sound & Vibration* 329 (8) 2010: pp. 980 – 993. https://doi.org/10.1016/j.jsv.2009.10.019
5. **Mohammadi, F., Sedaghati, R.** Vibration Analysis and Design Optimization of Viscoelastic Sandwich Cylindrical Shell *Journal of Sound & Vibration* 331 (12) 2012: pp. 2729 – 2752. https://doi.org/10.1016/j.jsv.2012.02.004
6. **Xu, Z., Huang, Q., Zhao, Z.** Topology Optimization of Composite Material Plate with Respect to Sound Radiation *Engineering Analysis with Boundary Elements* 35 (1) 2011: pp. 61 – 67. https://doi.org/10.1016/j.enganabound.2010.05.013
7. **Shojaeifard, M., Talebitooti, R., Yadollahi, A.** Optimization of Sound Transmission Through Laminated Composite Cylindrical Shells by Using a Genetic Algorithm *Mechanics of Composite Materials* 47 (4) 2011: pp. 481 – 494. https://doi.org/10.1007/s11029-011-9225-7
8. **Niu, B., Olhoff, N., Lund, E., Cheng, G.** Discrete Material Optimization of Vibrating Laminated Composite Plates for Minimum Sound Radiation *International Journal of Solids and Structures* 47 (16) 2010: pp. 2097 – 2114. https://doi.org/10.1016/j.ijsolstr.2010.04.008
9. **Abe, K., Fujiu, T., Koro, K.** A BE-based Shape Optimization Method Enhanced by Topological Derivative for Sound Scattering Problems *Engineering Analysis with Boundary Elements* 34 (12) 2010: pp. 1082 – 1091. https://doi.org/10.1016/j.enganabound.2010.06.017
10. **Assaf, S., Guerich, M., Cuvelier, P.** Vibration and Acoustic Response of Damped Sandwich Plates Immersed in a Light or Heavy Fluid *Computers & Structures* 88 (13 – 14) 2010: pp. 870 – 878. https://doi.org/10.1016/j.compstruc.2010.04.006
11. **Zhang, Z., Ni, X., Xu, Z., He, Y., Xu, X.** Research on Improvement of Cab Acoustic Characteristics Using

Damping Material *Journal of Mechanical Engineering* 48 (16) 2012: pp. 36. https://doi.org/10.3901/JME.2012.16.036

12. **Fan, Z., Wang, T., Yang, M.** Optimization of Non-local Impedance Parameters of Viscoelastic Materials *Journal of Beijing University of Aeronautics and Astronautics* 38 (2) 2012: pp. 268 – 272. https://doi.org/10.13700/j.bh.1001-5965.2012.02.014
13. **Chen, W., Liu, S.** Analysis and Design Optimization of Porous Materials for Sound Absorption *Noise and Vibration Control* 2012: pp. 288 – 293. https://doi.org/10.1007/s11783-011-0280-z
14. **Chen, L., Zhang, Y.** Composite Material Structural-acoustic Optimization Based on Genetic Algorithm *Acta Materiae Compositae Sinica* 29 (3) 2012: pp. 203 – 207. https://doi.org/10.13801/j.cnki.fhclxb.2012.03.033
15. **Wu, L., Yao, W.** Secondary Collaborative Optimization Design Method for Composite Reinforced Plate Structure *Journal of Nanjing University of Aeronautics and Astronautics* 43 (5) 2011: pp. 645 – 649. https://doi.org/10.3969/j.issn.1005-2615.2011.05.014
16. **Li, H., Chen, G., Zhang, B.** Topology Optimization Design of Structural Damping Plate Noise Reduction Considering Acoustic Vibration Coupling *Vibration Testing and Diagnosis* 31 (5) 2011: pp. 586 – 590. https://doi.org/10.3969/j.issn.1004-6801.2011.05.011
17. **Yang, M., Feng, T., Jia, Y., Wang, J.** Study on Mixed Calculation Method of Normal Sound Absorption Coefficient of Foam Material under Air Backing Condition *Noise and Vibration Control* 38 (2) 2018: pp. 42 – 76. https://doi.org/10.3969/j.issn.1006-1355.2018.02.009
18. **Su, J., Liu, W., Huang, N.** Research on Optimization of Acoustic Packaging Performance of Electric Vehicle Motor Compartment Based on Transfer Matrix Theory *Materials Science (Medžiagotyra)* In Press 2025: pp. 17. https://doi.org/10.5755/j02.ms.42507
19. **Gu, X., Huang, J., Jiang, Z., Qu, J., Zhong, Z.** Analysis of Factors Affecting the Sound Absorption Performance of Automotive Roof Lining *Automobile Technology and Materials* 11 2024: pp. 46 – 50. https://doi.org/10.19710/J.cnki.1003-8817.20230421
20. **Yang, W., Wen, J., Zhao, H., Wen, X.** Optimization Design of Automotive Acoustic Package Based on Material Parameter Inverse Inference *Chongqing University* 2023.
21. **Ali, M., Singh, B.** The Effect of Porosity on the Properties of Glass Fibre-reinforced Gypsum Plaster *Journal of Materials Science* 10 (11) 1975: pp. 1920 – 1928. https://doi.org/10.1007/BF00754481